

Nanoscale

Accepted Manuscript



This is an *Accepted Manuscript*, which has been through the Royal Society of Chemistry peer review process and has been accepted for publication.

Accepted Manuscripts are published online shortly after acceptance, before technical editing, formatting and proof reading. Using this free service, authors can make their results available to the community, in citable form, before we publish the edited article. We will replace this *Accepted Manuscript* with the edited and formatted *Advance Article* as soon as it is available.

You can find more information about *Accepted Manuscripts* in the [Information for Authors](#).

Please note that technical editing may introduce minor changes to the text and/or graphics, which may alter content. The journal's standard [Terms & Conditions](#) and the [Ethical guidelines](#) still apply. In no event shall the Royal Society of Chemistry be held responsible for any errors or omissions in this *Accepted Manuscript* or any consequences arising from the use of any information it contains.

COMMUNICATION

Self-assembly ultrathin Cu₂MoS₄ nanobelts for high efficient visible light-driven degradation of methyl orange

Ke Zhang[†], Wenxing Chen[†], Yunxiang Lin, Haiping Chen, Yasir A. Haleem, Chuanqiang Wu, Fei Ye, Tianxing Wang, Li Song*

National Synchrotron Radiation Laboratory, CAS Hefei Science Center, University of Science and Technology of China, Hefei, Anhui 230029, China

[†]These authors contributed equally to this work.

*Corresponding author: song2012@ustc.edu.cn

Abstract

We demonstrate an ultrathin self-assembled Cu₂MoS₄ nanobelt synthesized by using Cu₂O as the starting sacrificial template via a hydrothermal method. The nanobelts exhibit strong light absorption over a broad wavelength spectrum, suggesting its potential application as photocatalyst. The photocatalytic activity of nanobelts is evaluated by degradation of Methyl Orange dye (MO) under visible light irradiation. Notably, the nanobelts can completely degrade 100 mL 15 mg/mL MO in 20 minutes with excellent recycling and structural stability, suggesting its excellent photocatalytic performance. In comparison with sheet-like sample, the high efficiency of self-assembled Cu₂MoS₄ nanobelts is attributed to high surface area and unique band gap, agreeing with the nitrogen adsorption analysis and photoluminescence spectra. This study offers a self-assembly synthetic route to create new multifunctional nanoarchitectures composed of atomic layers, thus may open a window for greatly extending potential applications in water pollutant treatment, photocatalytic water-splitting, solar cells and other related fields.

1. Introduction

The research of photocatalytic and photoelectrocatalytic feature of various nanomaterials not only provides useful insights to fundamental questions of photochemistry and photoelectrochemistry, but also creates next-generation catalysts.¹⁻³ During the past years, tremendous efforts have been made to resolve the increasingly serious energy and environment problems by exploring various solar-driven photocatalysts.^{4,5} Irrespective of traditional photocatalytic materials, such as TiO₂⁶⁻⁹ and ZnO,^{10,11} some new photocatalysts have been developed in order to extend the absorption range to visible-light region. In particular, plasmonic-enhanced photocatalysts¹² have been recently studied as promising visible-light-absorbing materials, i.e. Ag@AgCl,¹³ Cu₂O-Au hybrid structure.¹⁴ However, the use of noble metal (Ag, Au) in these photocatalysts causes the high cost, limiting their practical applications. The booming of graphene has brought new opportunities for hybrid photocatalysis,^{15,16} but the ideal formation of graphene compositions is usually inconvenient, and the controllable construction on robust interface between graphene and active materials is still a big challenge, which seriously influences their photocatalytic activity and durability. So it is crucial to explore new photocatalysts which are not only facilely-prepared and well-stable, but also earth-abundant and environment-friendly.

Among various candidates, transition metal sulphides (TMSs) are one of ideal catalysts because of their excellent absorption on visible-light region and extensive source, especially ternary transition metal sulphides (TTMS) nanomaterials.^{17,18} Until now, amount of efforts have been put into exploring different approaches to enhance the photocatalytic performance of TTMS materials, such as ZnIn₂S₄,¹⁹ CuInS₂.²⁰ As one of typical TTMS, ternary Cu₂MoS₄ is known as an earth-abundant, environment-friendly and low-cost semiconductor material.^{21,22} It has been demonstrated by Guo *et al.* that Cu₂MoS₄ material had intensive absorption in visible light region, which is predictive to exhibit good performance in visible-light-driven photocatalysis.²³ Recently, Tran *et al.* successfully synthesized Cu₂MoS₄ samples as novel electro- and photoelectro- catalysts for hydrogen evolution reaction (HER). The excellent catalytic performance of Cu₂MoS₄ is ascribed to accelerate the multi-electronic nature of chemical reactions in HER.²⁴ However, it's still a problem to prepare Cu₂MoS₄ samples with high surface area, high uniformity and no-impurity for further enhancing their catalytic efficiency.

Herein, we successfully prepared self-assembled Cu₂MoS₄ (space group I42m) nanobelt via a modified hydrothermal method. And their photocatalytic behavior for the degradation of Methyl Orange dye (MO) under visible-light irradiation were investigated. The photocatalytic tests revealed that the nanobelts exhibited excellent photocatalytic performance by degrading 100 mL 15 mg/mL MO in 20 min completely. Compared with our previous sheet-like sample,²⁵ the according reasons for the high efficiency of Cu₂MoS₄ nanobelt are further discussed. Thanks to its unique bundle-assembled structure, the ultrathin Cu₂MoS₄ nanobelt show higher surface areas and visible light absorption in contrast to the sheet-like sample. Meanwhile, the weaker photoluminescence spectra of the nanobelt further confirmed its better efficiency of separation of photogenerated electron-hole pairs. This work offers a common method to prepare Cu₂MX₄ (M=Mo, W; X=S, Se) nanomaterials with various

morphologies and also provides useful insights for designing other excellent catalysts for many specific applications.

2. Experimental section

The Cu_2MoS_4 nanobelts are synthesized using a modified hydrothermal method based on our previous work.²⁴ First of all, 40 mg Cu_2O powder was dispersed in 25 ml deionized water by sonication for 5 min, then 108 mg $(\text{NH}_4)_2\text{MoS}_4$ was dissolved in the solution. After stirring for 5 min, the precursor was transferred into a 45 mL Teflon-lined stainless steel autoclave and maintained at 160 °C for 9 h. The final products were washed with deionized water and ethanol for several times to remove any possible ions, and then dried at 60 °C under vacuum for a couple of hours.

The composition and structure of the as-prepared products were characterized by X-ray powder diffraction (XRD, Philips X' Pert Pro Super X-ray diffractometer $\text{Cu K}\alpha$ ($\lambda=1.54178$ Å) radiation). The morphologies were observed by a scanning electron microscope (SEM, JSM-6700F, and 5 kV) and a transmission electron microscope (TEM, JEOL JEM-2100F microscope, 200 kV). Energy dispersive X-ray (EDX) element mapping analysis was carried out in a JEOL ARM-200 microscope at 200 kV. The samples were dispersed in ethanol and dropped onto a gold grid with a carbon film coated for TEM characterizations. The AFM analysis was carried out using Veeco MultiMode V. The UV-vis spectra were taken using a Shimadzu DUV-3700 spectrophotometer. N_2 sorption isotherms were recorded with a surface area and pore size analyzer (Micromeritics Tristar 3020). All of the samples were degassed under vacuum for 12 h before measurements. The specific surface area was calculated by the Brunauer–Emmett–Teller (BET) method using adsorption data. The photoluminescence spectra of the samples were recorded on a Jobin Yvon Horiba Fluorolog-3-Tau Spectrofluorometer.

The photocatalytic activities of the Cu_2MoS_4 samples were evaluated by degradation dyes of methylene orange (MO) under 300 W Xe lamp with UV cut-off filter (providing visible light with a wavelength longer than 420 nm). The samples (20 mg, 50 mg) were put into a solution of MO (100 mL, $15 \text{ mg}\cdot\text{L}^{-1}$) in a 200 mL glass beaker. Before the lamp was switched on, the solution was stirred in the dark for 120 min to ensure adsorption/desorption equilibrium between Cu_2MoS_4 and dye. Under constant stirring, about 5 mL of the mixture solution was taken out at different intervals. After centrifugation, the UV/Vis spectrum of the supernatant was recorded to monitor the degradation behaviour.

3. Results and discussion

Fig. 1A is EDX spectrum of the obtained samples, indicating the presence of Cu, Mo and S elements. Whereas, Fig. 1B shows the corresponding powder X-ray diffraction (XRD) patterns. According to previous reports, the XRD peaks can be well assigned Cu_2MoS_4 with I-phase.²⁵ Notably, no peak is observed for impurities (i.e. MoS_2 or Cu_2S), indicating that the as-prepared sample is highly crystalline and pure quality of Cu_2MoS_4 .

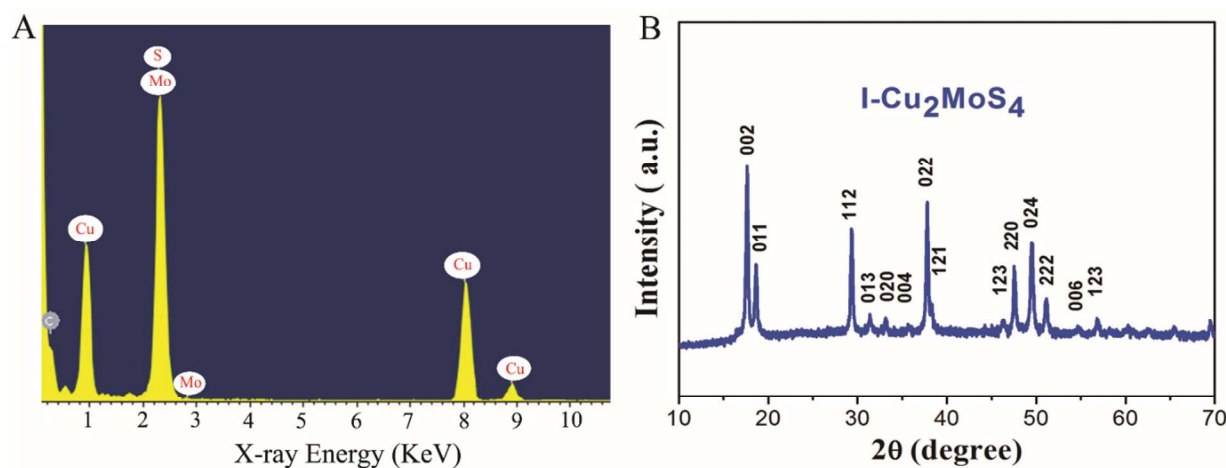


Fig. 1 A) EDX Spectrum and B) XRD patterns of as-prepared Cu₂MoS₄ nanobelt.

Fig. 2A and 2B show representative SEM and TEM images of the obtained Cu₂MoS₄ samples, respectively. It is noted that the samples exhibit uniform bundle structure with no particle-like impurity. The average length and width of the bundle is 1-1.5 μm and 50-100 nm. The typical TEM image in Fig. 2B reveals that the resulting products are composed mainly of belt-like nanostructures with well-defined facets. The high-resolution TEM (HRTEM) analysis in Fig. 2C further confirms the highly crystalline nature of nanobelt. The crystal lattices of 2.72 Å and 1.91 Å correspond to the d-spacing of both (200) and (220) facets. The selected-area electron diffraction (SAED) pattern is shown in Fig. 2D, which reveals that the nanobelt was single crystal. To accurately detect the thickness of the nanobelt, atomic force microscopy (AFM) analysis was done in tapping-mode (see Fig. S1 in Supplementary Information). The AFM profile calculation of the nanobundle shows the thickness range of 5-25 nm, suggesting that the nanobundles are formed by the stack of several ultrathin nanobelts. In addition, Fig. 2E shows the elemental mapping of the samples. It can be seen that Cu, Mo, and S are uniformly distributed within the samples. The calculated molar ratio of Cu: Mo: S is about 2:1.1:4, further suggesting the as-prepared Cu₂MoS₄.

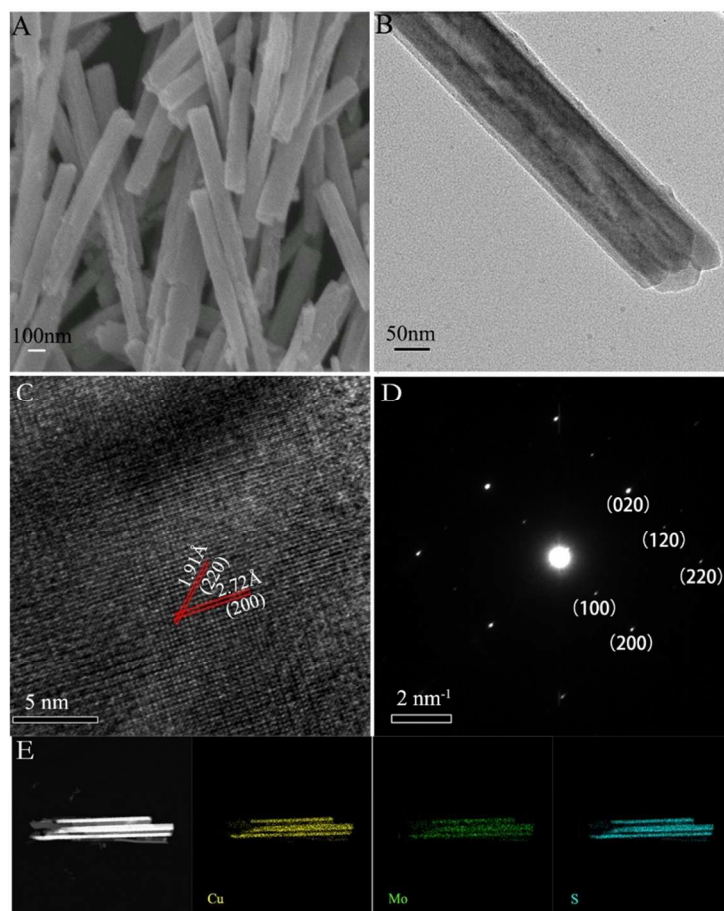


Fig. 2 Electron microscope characterizations of the self-assembling Cu_2MoS_4 nanobelt. A) Typical SEM and B) TEM images. C) High-resolution TEM image. D) Selected area electron diffraction patterns. E) Elemental mapping images of Cu, Mo, and S, respectively.

For better understanding of the growth mechanism of Cu_2MoS_4 nanobelt, time-dependent experiments were carried out by preparing samples at different reaction times (0 h, 3 h, 6 h, 9 h, 12 h), then characterized by TEM and SEM. The results are shown in Fig. 3A (also see Fig. S3 in Supplementary Information). It can be observed that the starting Cu_2O materials, acting as sacrificial template, exhibit the size from 100 to 200 nm with sphere-like morphology. Further, dispersion of Cu_2O nanosphere in deionized water, followed by hydrothermal reaction can change them to a hollow-sphere structure. Meanwhile, some branches can also be formed on the surface of hollow-sphere (like a meteor hammer). It is noted that with the increasing of reaction time, the length of branches can be continuously grown and self-assembled into nanobundles. Finally, the sacrificial Cu_2O hollow-sphere is fractured, and the fall-off nanobundles can attach each other to form the stacking nanobelts. Above mentioned experimental observations, may suggest synthetic route for the formation of Cu_2MoS_4 nanobelts, as illustrated in Fig. 3B. During the synthesis of Cu_2MoS_4 nanobelts, free MoS_4^{2-} ions in the solution tend to react with Cu_2O and form Cu_2MoS_4 at the surface of nanosphere. After a 3-hour hydrothermal process, the hollow structure are formed because of Kirkendall effect.²⁶ By controlling the reaction parameters, we can selectively achieve the oriented growth of Cu_2MoS_4 nanobelts along the (100) crystal direction.

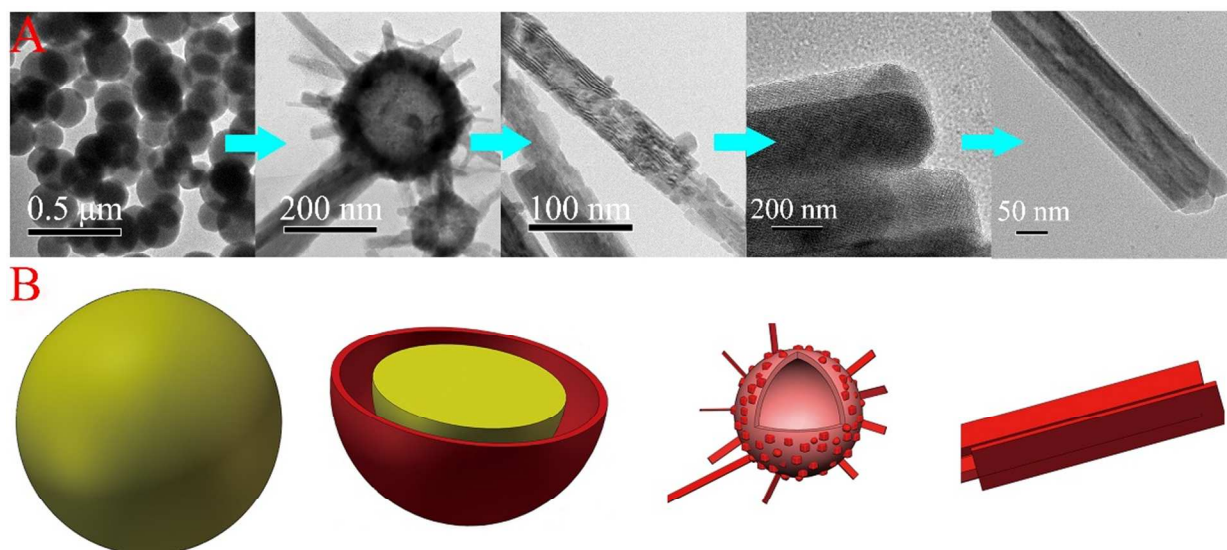


Fig. 3 A) TEM images of various samples at different reaction times (0 h, 3 h, 6 h, 9 h, 12 h). B) The schematic illustration proposes the growth formation of Cu_2MoS_4 nanobelt.

The UV-vis diffuse reflectance spectra of nanobelt is shown in Fig. 4A. The nanobelts exhibit an enhanced strong light absorption in the wavelength range of 300-800 nm. The photographs of samples dispersed in ethanol are shown in the inset of Fig. 4A. It can be seen that the nanobelt solution displays bright-red colour. The unique behaviors of strong light absorption and well dispersion motivate us to investigate the obtained Cu_2MoS_4 nanobelt as potential photocatalysis.

The photocatalytic activity of the as-prepared samples was investigated by photodegradation of Methyl Orange (MO) under visible light irradiation. As shown in Fig. 4B, the blank experiment shows that the MO degradation without catalysts contributes a little under visible light, while the nanobelts exhibited excellent photocatalytic activity. By adding 20 mg Cu_2MoS_4 nanobelt in the 100 mL 15mg/mL MO, 95% MO dye can be degraded in 60 min. What's more, by adding 50 mg Cu_2MoS_4 nanobelt, 90% MO dye can be degraded within 15 min, and completely degraded in 20 min. As the best of our knowledge, this means that the ultrathin Cu_2MoS_4 nanobelt is one of the most efficient photocatalysts for MO degradation under visible-light irradiation, sometimes even more efficient than some high-cost photocatalysts, like Ag_3PO_4 (i.e. 200 mg Ag_3PO_4 nanosphere catalyst were put into a solution of 100 mL 8 mg/mL, and the dye were completely degraded in 28 min).²⁷ Thus, we suggest that the Cu_2MoS_4 nanobelt can be one of ideal photocatalysts for MO degradation in combination with low-cost, low-dosage and high efficiency.

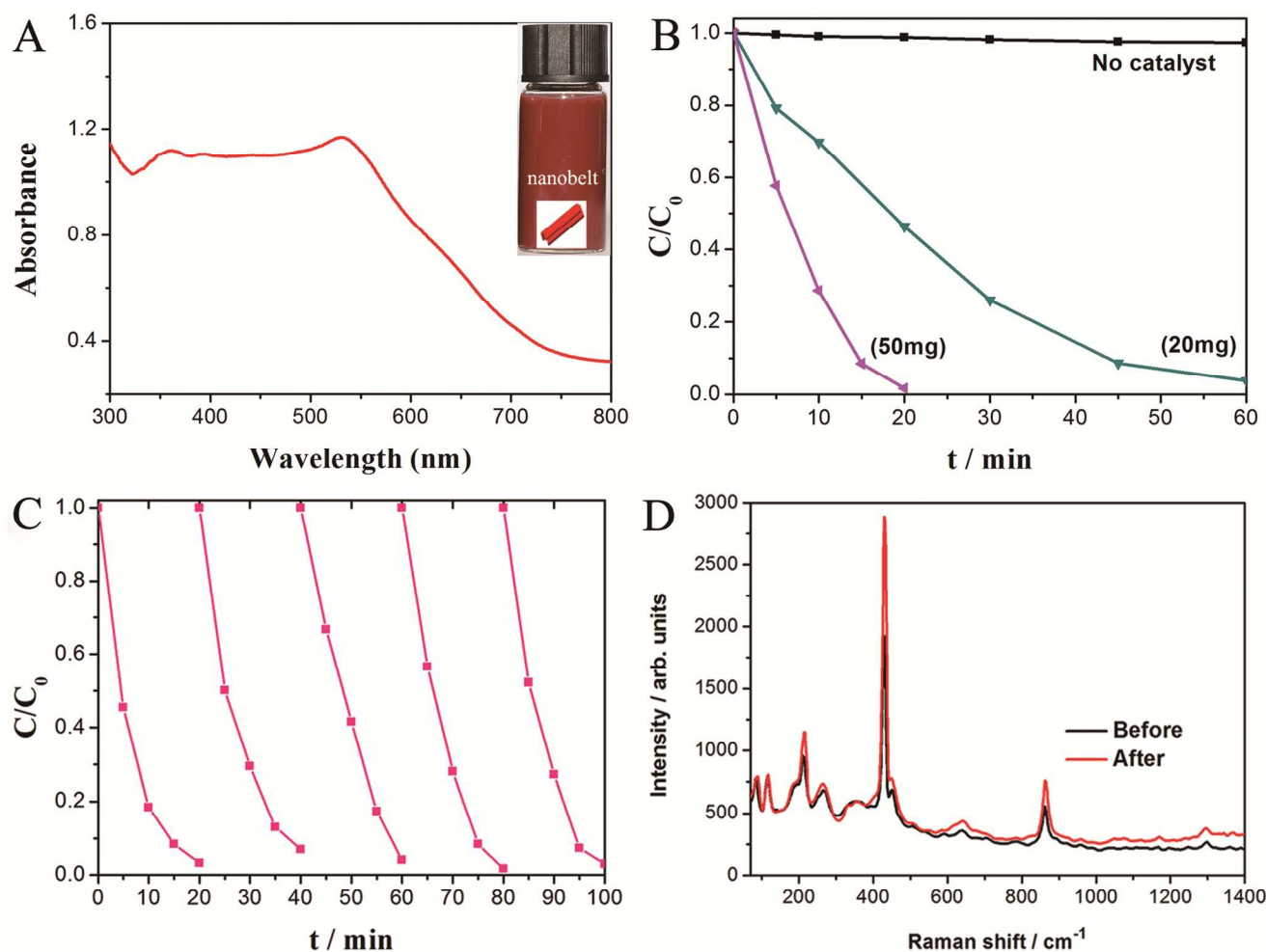


Fig. 4 A) Diffuse reflectance absorption spectra of Cu_2MoS_4 nanobelt. The inset shows the photograph of the sample dispersed in ethanol. B) Photocatalytic activities of Cu_2MoS_4 nanobelt for MO degradation under visible-light irradiation ($\lambda > 420$ nm). C) Visible light-driven degradation of MO repeated cycles in 100 min by Cu_2MoS_4 nanobelt. D) Raman spectra of the nanobelts before and after tens of MO degradation cycling, the excited laser wavelength is 532 nm.

Apart from high photocatalytic activity, other important factors of new photocatalyst for many practical applications is the recycling performance and stability. The recycling performance of the nanobelt were shown in Fig. 4C. After five recycles, it still shows similar catalytic efficiency to first recycle. In order to evaluate the structural stability, Raman spectroscopy was performed on the samples before and after degradation. Fig. 4D shows a comparative spectrum of the nanobelts before and after tens of photodegradation treatments. The main peaks can be assigned to four Raman active modes, similar to our previous report.²⁸ It is noted that no obvious change is found in comparison of the Raman peaks recorded before and after degradation, which strongly suggests the good structural stability of the nanobelts even after many catalytic reactions.

In order to explain underlying mechanism for excellent photocatalytic activity of the self-assembled Cu_2MoS_4 nanobelt, we carried out a comparison study by selecting sheet-like Cu_2MoS_4 as control sample. The results for Cu_2MoS_4 nanosheet are shown in the Supplementary Information (See Fig. S3 and S4). In contrast to Cu_2MoS_4 nanobelt, the sheet-like sample exhibit comparable worse visible light absorption ability (the colour of the nanosheet dispersed in ethanol is dark-red). More notably, the calculated photodegradation efficiency for Cu_2MoS_4 nanobelt is about 7.5 times (20 mg catalyst) and 6 times (50 mg catalyst) comparing with sheet-like sample. It is known that the large specific surface areas of the photocatalyst benefits the photocatalytic activity.²⁹ The Brunauer-Emmett-Teller (BET) nitrogen adsorption analysis were performed on the two samples. Fig. 5A shows that the specific surface area of Cu_2MoS_4 nanobelt is around $35.4 \text{ m}^2\text{g}^{-1}$, which is 2.6 times larger than that of sheet-like sample. Another important factor for photocatalytic performance is the recombination of excited electrons and holes. Photoluminescence (PL) emission is used to obtain the separation efficiency of the photogenerated of electrons and holes. As shown in Fig. 5B, the PL spectra of both samples exhibit emission peaks in the 300-800 nm range under the excitation at 320 nm. In comparison with sheet-like sample, self-assembled Cu_2MoS_4 nanobelt show weaker PL intensity, indicating its better efficiency for separating the photogenerated of electrons and holes. In addition, the comparable small thickness may also contribute to good photocatalytic activity in Cu_2MoS_4 nanobelt. Guo *et al.* have changed the ratio of (001)/(101) facets by controlling the thickness of Cu_2WS_4 decahedra via PVP-assisted hydrothermal method.³⁰ And the change of (001)/(101) should play a more important role in its photoreactivity. In this condition, the ultrathin Cu_2MoS_4 nanobelt may show higher ratio of high energy surface than nanosheet.

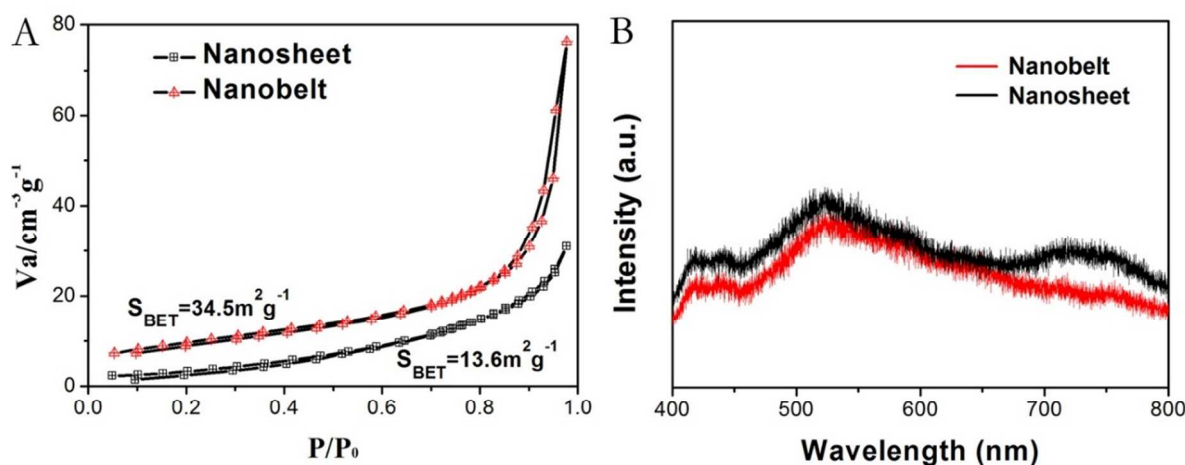


Fig. 5 A) The nitrogen adsorption-desorption isotherm of Cu_2MoS_4 nanobelts (upside) and nanosheets (bottom) show that the BET surface areas are about $34.5 \text{ m}^2\text{g}^{-1}$ and $13.6 \text{ m}^2\text{g}^{-1}$, respectively. B) Photoluminescence spectra of the two samples, the excited laser wavelength is 325 nm

4. Conclusion

Ultrathin self-assembled Cu_2MoS_4 nanobelt with the length of several microns and the thickness of 5-25 nm were successfully synthesized by a hydrothermal method. Our characterizations revealed that nanobelt was composed of numerous stacked Cu_2MoS_4 layers with belt-like morphology. The time-dependent experiments indicate that free MoS_4^{2-} ions in the solution tend to react with Cu_2O to form small Cu_2MoS_4 branches at the surface of Cu_2O hollow-sphere structures because of Kirkendall effect. It is worth mentioning that as time passes during hydrothermal reaction, the small branches were grown into the nanobundles. These nanobundles fall off and self-assembled to form the final stacking nanobelts. The visible light-driven photocatalytic performance of the as-obtained nanobelts was investigated systematically. Owing to the strong visible light absorption, large specific surface areas and low recombination of excited charges, Cu_2MoS_4 nanobelt exhibited excellent photocatalytic activity, even better than some high-cost noble metal-photocatalysts. Meanwhile, the nanobelts also showed good recycle performance and durability. The presented results can provide a new self-assembly route to selectively prepare new multifunctional layered nanostructures with high surface area and rich active edges, thus greatly extend their potential applications in catalytic and new energy related fields.

Acknowledgements

This work was financially supported by the National Basic Research Program of China (2014CB848900), the National Natural Science Foundation of China (U1232131, 11375198) and the Fundamental Research Funds for the Central Universities (WK2310000035). We thank the Shanghai synchrotron Radiation Facility (14W1, SSRF), the Beijing Synchrotron Radiation Facility (1W1B, BSRF) and the NSRL soft-X-ray endstation for helps in characterizations. L.S. thanks the recruitment program of global experts and the CAS Hundred Talent Program of China.

Notes and references

- 1 A. Fujishima, *Nature*, 1972, **238**, 37-38.
- 2 H. Tong, S. X. Ouyang, Y. P. Bi, N. Umezawa and M. Oshikiri, J. H. Ye, *Adv. Mater.*, 2012, **24**, 229-251.
- 3 H. M. Chen, C. K. Chen, R. S. Liu, L. Zhang, J. J. Zhang and D. P. Wilkinson, *Chem. Soc. Rev.*, 2012, **41**, 5654-5671.
- 4 H. F. Cheng, B. B. Huang and Y. Dai, *Nanoscale*, 2014, **6**, 2009-2026.
- 5 H. Wang, J. T. Yang, X. L. Li, H. Z. Zhang, J. H. Li and L. Guo, *Small*, 2012, **8**, 2802-2806.
- 6 X. B. Chen and S. S. Mao, *Chem. Rev.*, 2007, **107**, 2891-2959.
- 7 X. B. Chen, S. H. Shen, L. J. Guo and S. S. Mao, *Chem. Rev.*, 2010, **110**, 6503-6570.
- 8 X. B. Chen, L. Liu, P. Y. Yu and S. S. Mao, *Science*, 2011, **331**, 746-750.
- 9 H. G. Yang, C. H. Sun, S. Z. Qiao, J. Zou, G. Liu, S. C. Smith, H. M. Cheng and G. Q. Lu, *Nature*, 2008, **453**, 638-641.

- 10 K. Maeda, T. Takata, M. Hara, Nobuo Saito, Y. Inoue, H. Kobayashi and K. Domen, *J. Am. Chem. Soc.*, 2005, **127**, 8286-8287.
- 11 B. Weintraub, Z. Z. Zhou, Y. H. Li and Y. L. Deng, *Nanoscale*, 2010, **2**, 1573-1587.
- 12 S. Linic, P. Christopher and D. B. Ingram, *Nature Materials*, 2011, **10**, 911-921.
- 13 P. Wang, B. B. Huang, X. Y. Qin, X. Y. Zhang, Y. Dai, J. Y. Wei and M. H. Whangbo, *Angew. Chem. Int. Ed.*, 2008, **47**, 7931-7933.
- 14 C. H. Kuo, T. E. Hua and M. H. Huang, *J. Am. Chem. Soc.*, 2009, **131**, 17871-17878.
- 15 Q. J. Xiang, J. G. Yu and M. Jaroniec, *Chem. Soc. Rev.*, 2012, **41**, 782-796.
- 16 H. Wang, H. B. Feng and J. H. Li, *Small*, 2014, **10**, 2165-2181.
- 17 S. L. Shen and Q. B. Wang, *Chem. Mater.*, 2013, **25**, 1166-1178.
- 18 C. H. Lai, M. Y. Yu and L. J. Chen, *J. Mater. Chem.*, 2012, **22**, 19-30.
- 19 L. Shang, C. Zhou, T. Bian, H. J. Yu, L. Z. Wu, C. H. Tung and T. R. Zhang, *J. Mater. Chem.*, 2013, **1**, 4552-4558.
- 20 L. Zheng, Y. Xu, Y. Song, C. Z. Wu, M. Zhang and Yi Xie, *Inorg. Chem.*, 2009, **48**, 4003-4009
- 21 C. Yang, P. D. Tran, P. P. Boix, P. S. Bassi, N. Yantara, L. H. Wong and J. Barber, *Nanoscale*, 2014, **6**, 6506-6510.
- 22 D. Y. Yu, R. L. Lee, R. Yi, S. Y. Chi and P. D. Tran, *Electrochimica Acta*, 2014, **115**, 337-343.
- 23 H. R. Liang and L. J. Guo, *Int. J. Hydrogen Energy.*, 2010, **35**, 7104-7109.
- 24 P. D. Tran, M. Nguyen, S. S. Pramana, A. Bhattacharjee, S. Y. Chiam, J. Fize, M. J. Field, V. Artero, L. H. Wong, J. Loo and J. Barber, *Energy Environ. Sci.*, 2012, **5**, 8912-8916.
- 25 W. X. Chen, H. P. Chen, H. T. Zhu, Q. Q. Gao, J. Luo, Y. Wang, S. Zhang, K. Zhang, C. M. Wang, Y. J. Xiong, Y. F. Wu, X. S. Zheng, W. S. Chu, L. Song and Z. Y. Wu, *Small*, 2014, **10**, 4637-4644.
- 26 W. S. Wang, M. Dahl and Y. D. Yin, *Chem. Mater.*, 2013, **25**, 1179-1189.
- 27 Y. P. Bi, S. X. Ouyang, N. Umezawa, J. Y. Gao and J. H. Ye, *J. Am. Chem. Soc.*, 2011, **133**, 6490-6492.
- 28 H. P. Chen, K. Zhang, W. X. Chen, I. Ali, P. Wu, D. B. Liu and L. Song, *AIP Advances*, 2015, **5**, 037141.
- 29 N. Zhang, S. X. Ouyang, T. Kako and J. H. Ye. *Chem. Commun.*, 2012, **48**, 9894-9896.
- 30 N. Li, M. C. Liu, Z. H. Zhou, J. C. Zou, Y. M. Sun and L. J. Guo. *Nanoscale*, 2014, **6**, 9695-9702